Neutral and methylated cationic Re(I) tetrazolato complexes: comparative photophysics, transient Raman spectroscopy and fabrication of OLED and LEEC devices

Melissa V. Werrett,[a,b] Gregory S. Huff,[c] Sara Muzzioli,[b] Valentina Fiorini,[b] Stefano Zacchini,[b] Brian W. Skelton,[d] Antonio Maggiore,[e] Joanna M. Malicka,[e] Massimo Cocchi,[e,f] Keith C. Gordon,[c] Stefano Stagni,[b,*] Massimiliano Massi[a,*]

[a] Department of Chemistry, Curtin University, Kent Street, Bentley WA 6102, Australia.

[b] Department of Industrial Chemistry, University of Bologna, viale del Risorgimento 4, 40126 Bologna, Italy.

[c] Department of Chemistry, University of Otago, Union Place, Dunedin, New Zealand.

[d] Centre for Microscopy, Characterisation and Analysis, University of Western Australia, Crawley 6009 WA, Australia.

[e] Consorzio MIST E-R Via P. Gobetti 101, 40129 Bologna, Italyf

[f] Institute for Organic Synthesis and Photoreactivity, CNR, via Gobetti 101, 40129 Bologna.

Electronic Supplementary Information

X-ray Structural Determinations

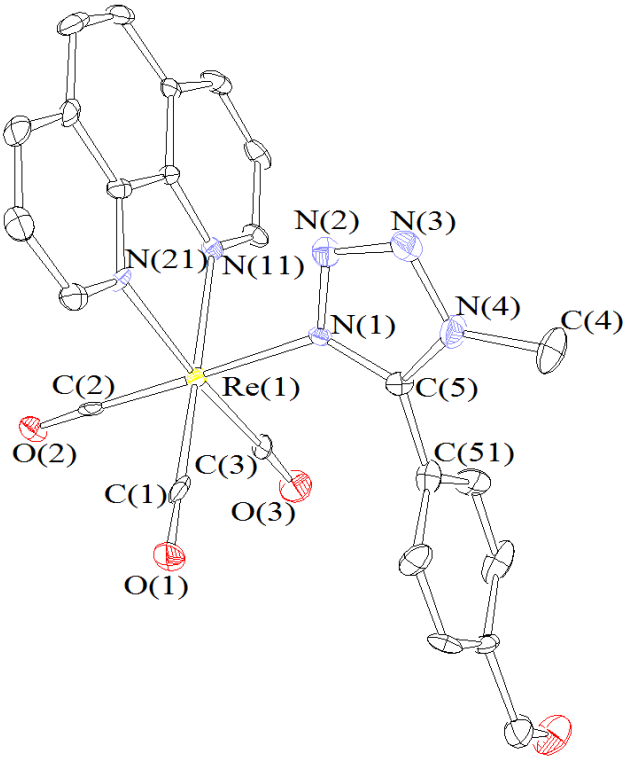

Figure S1. Molecular structure of *fac*-[Re(**phen**)$(CO)_3$(**Tbdz**CH_3)]$^+$ with key atoms labelled. Displacement ellipsoids are at 30 % probability level. H-atoms have been omitted for clarity.

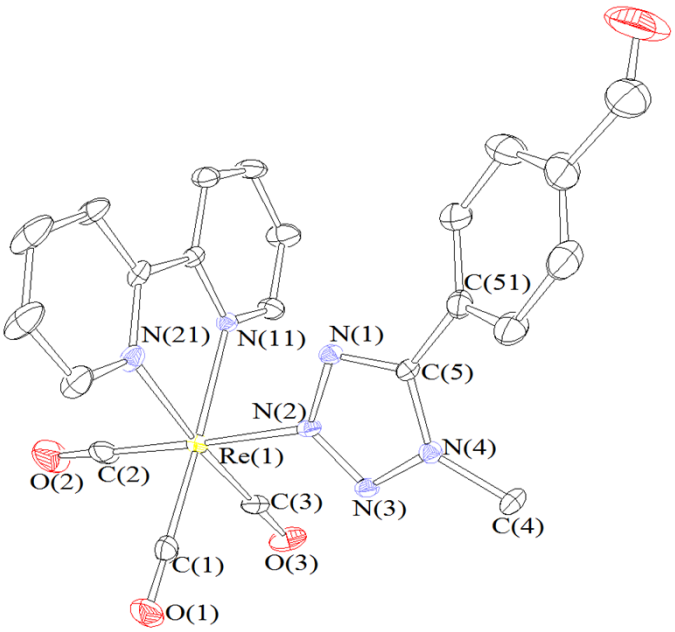

Figure S2. Molecular structure of *fac*-[Re(**bipy**)$(CO)_3$(**Tbdz**CH_3)]$^+$ with key atoms labelled. Displacement ellipsoids are at 30 % probability level. H-atoms have been omitted for clarity.

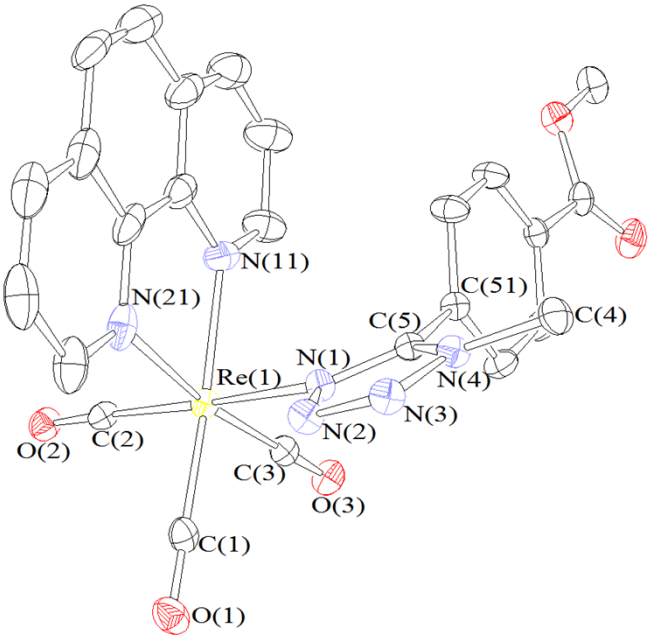

Figure S3. Molecular structure of *fac*-[Re(**phen**)$(CO)_3$(**Tmeb**CH_3)]$^+$ with key atoms labelled. Displacement ellipsoids are at 30 % probability level. H-atoms have been omitted for clarity.

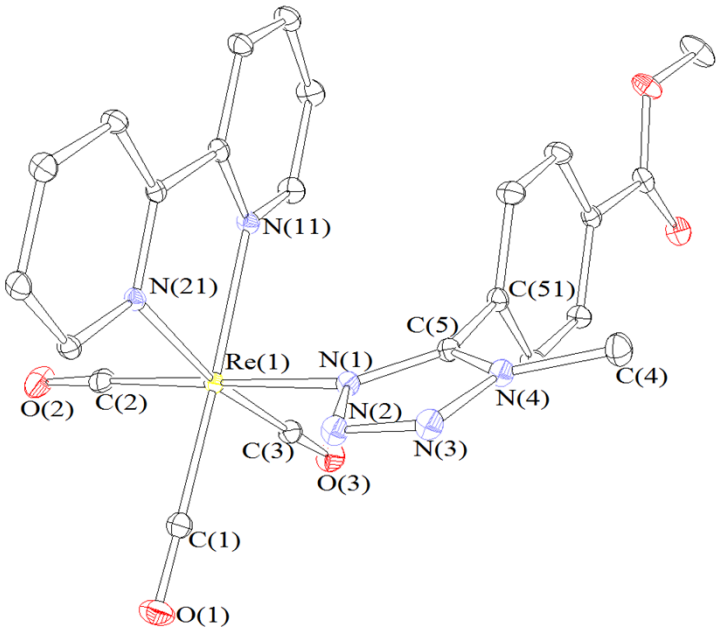

Figure S4. Molecular structure of *fac*-[Re(**bipy**)$(CO)_3$(**Tmeb**CH_3)]$^+$ with key atoms labelled. Displacement ellipsoids are at 30 % probability level. H-atoms have been omitted for clarity.

Absorption Spectra

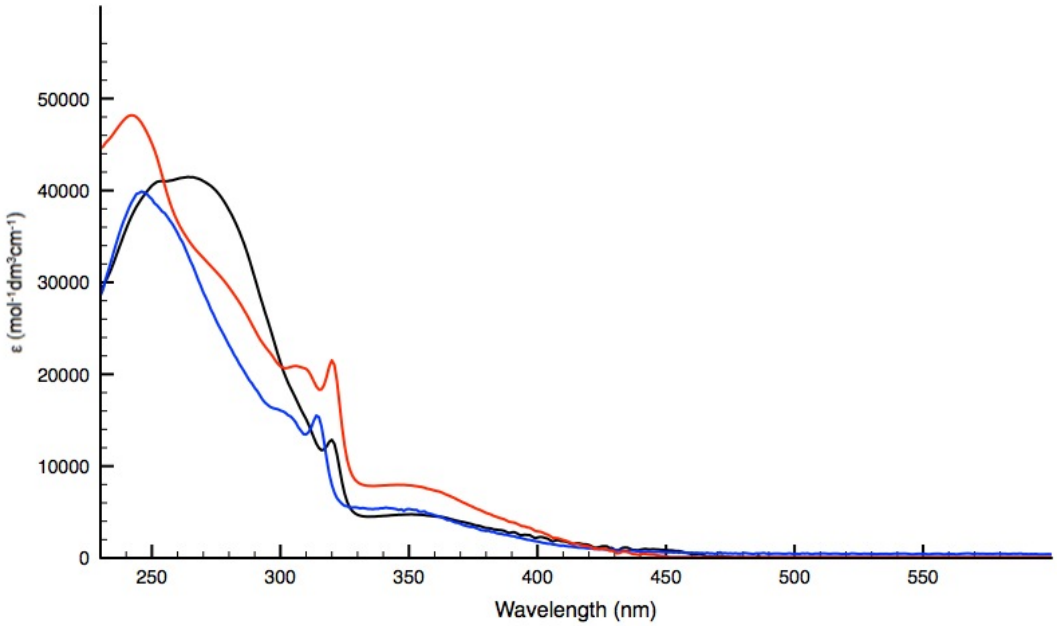

Figure S5. Absorption spectra of dichloromethane solutions (ca. 10^{-5} M) of the *fac*-[Re(**bipy**)$(CO)_3$(**L**)][PF_6] complexes, where **L** = **Tph**CH_3 (red trace), **Tbdz**CH_3 (blue trace) and **Tmeb**CH_3 (black trace).

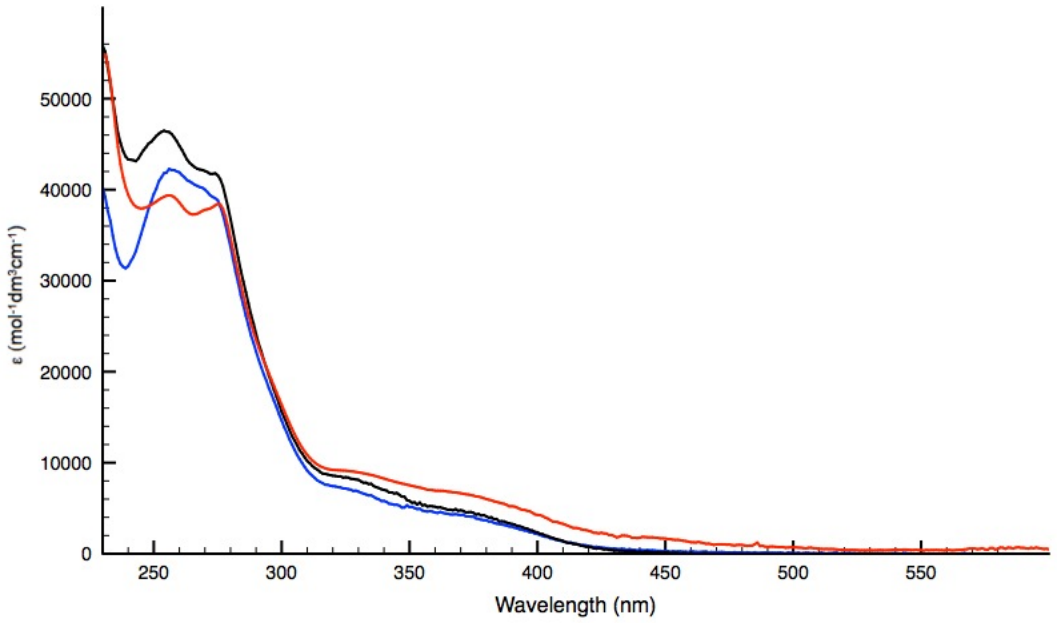

Figure S6. Absorption spectra of dichloromethane solutions (ca. 10^{-5} M) of the *fac*-[Re(**phen**)$(CO)_3$(**L**)][PF_6] complexes, where **L** = **Tph**CH_3 (red trace), **Tbdz**CH_3 (blue trace) and **Tmeb**CH_3 (black trace).

Emission Spectra at RT and 77 K

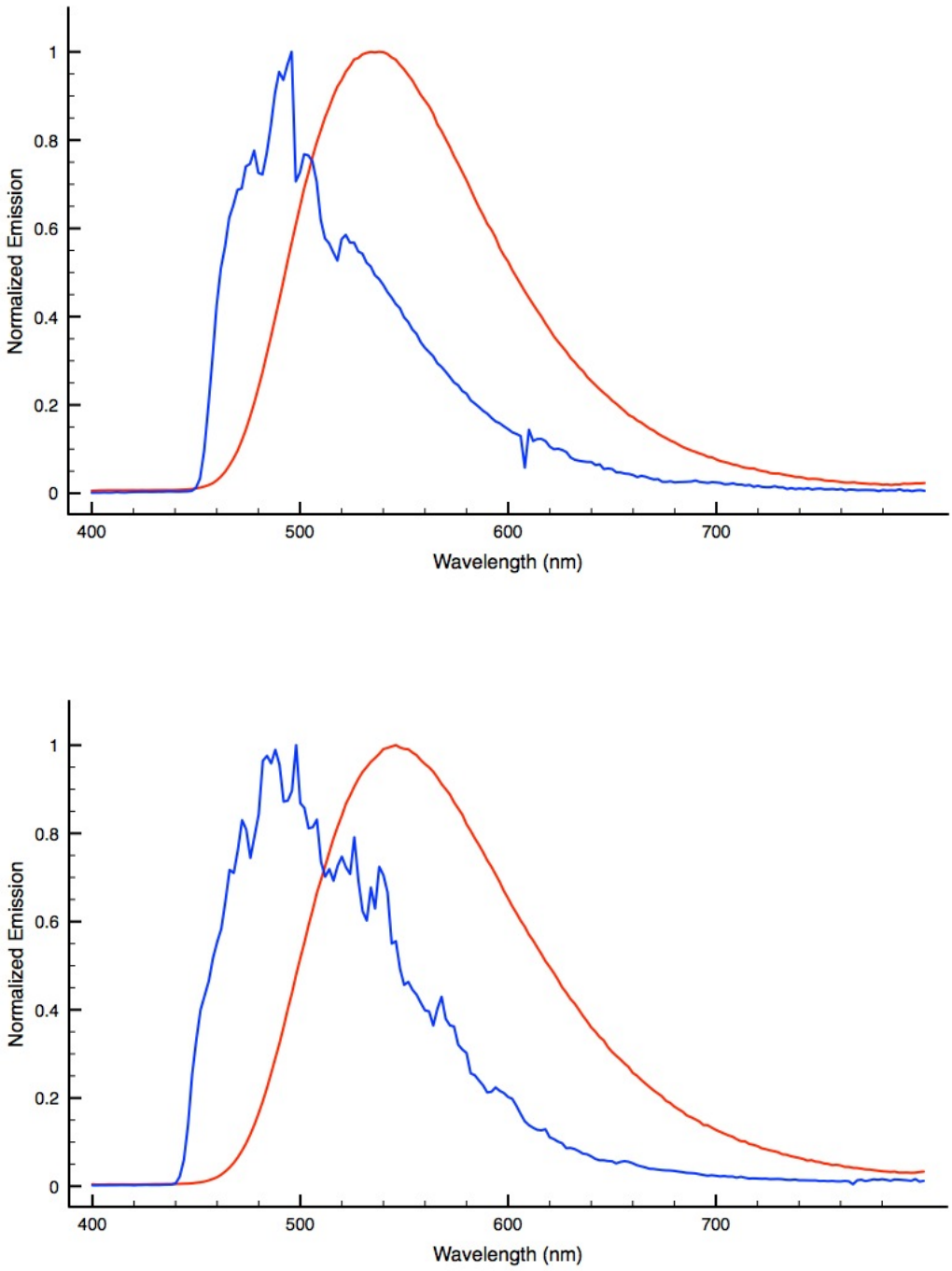

Figure S7 Comparison of the emission spectra obtained from dichloromethane fluid solutions at RT (red trace) and 77 K (blue trace) containing *fac*-[Re(**phen**)$(CO)_3$(**Tph**CH_3)][PF_6] (top) and *fac*-[Re(**bipy**)$(CO)_3$(**Tph**CH_3)][PF_6], (bottom).

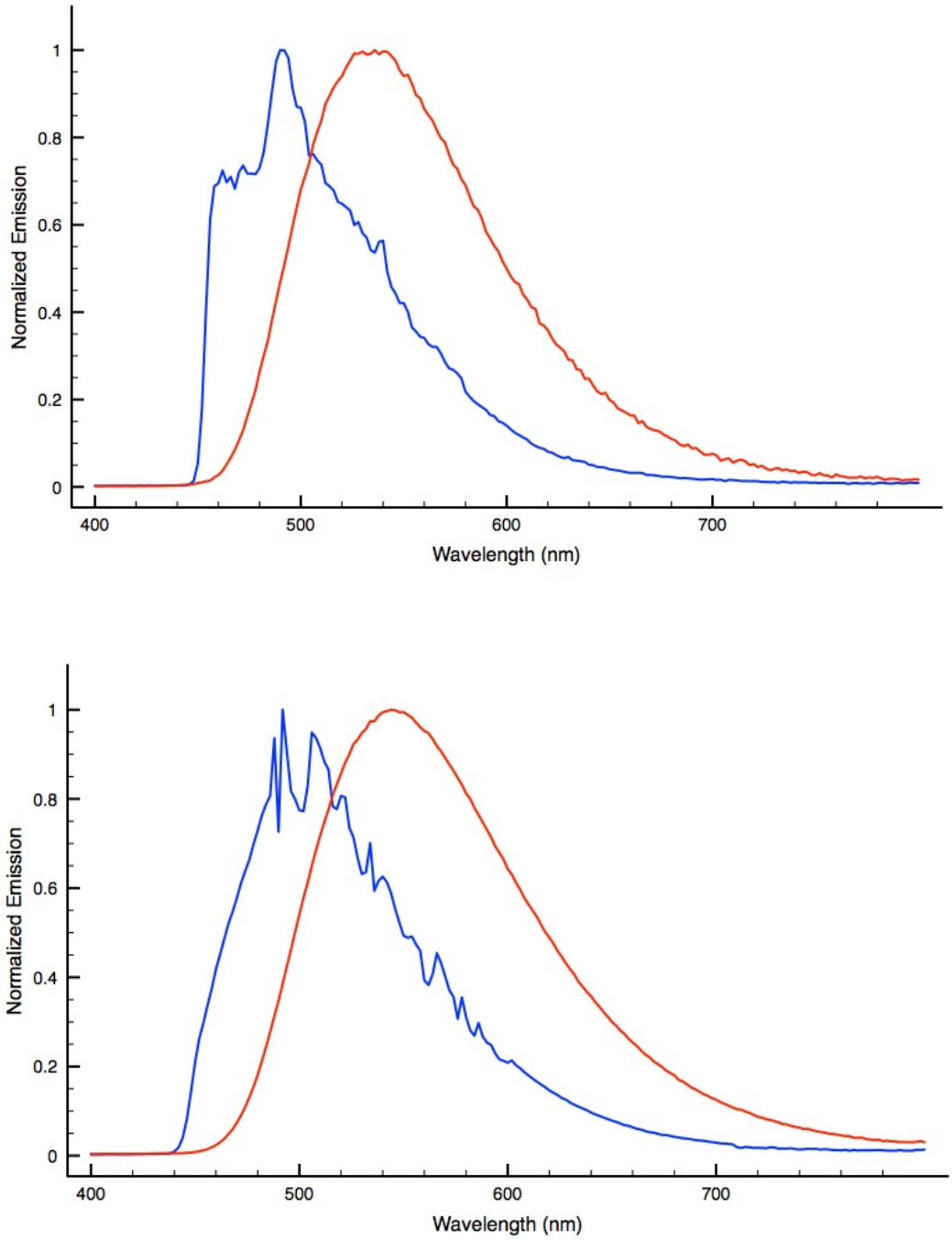

Figure S8. Comparison of the emission spectra obtained from dichloromethane fluid solutions at RT (red trace) and 77 K (blue trace) containing *fac*-[Re(**phen**)$(CO)_3$(**Tbdz**CH_3)][PF_6] (top) and *fac*-[Re(**bipy**)$(CO)_3$(**Tbdz**CH_3)][PF_6], (bottom).

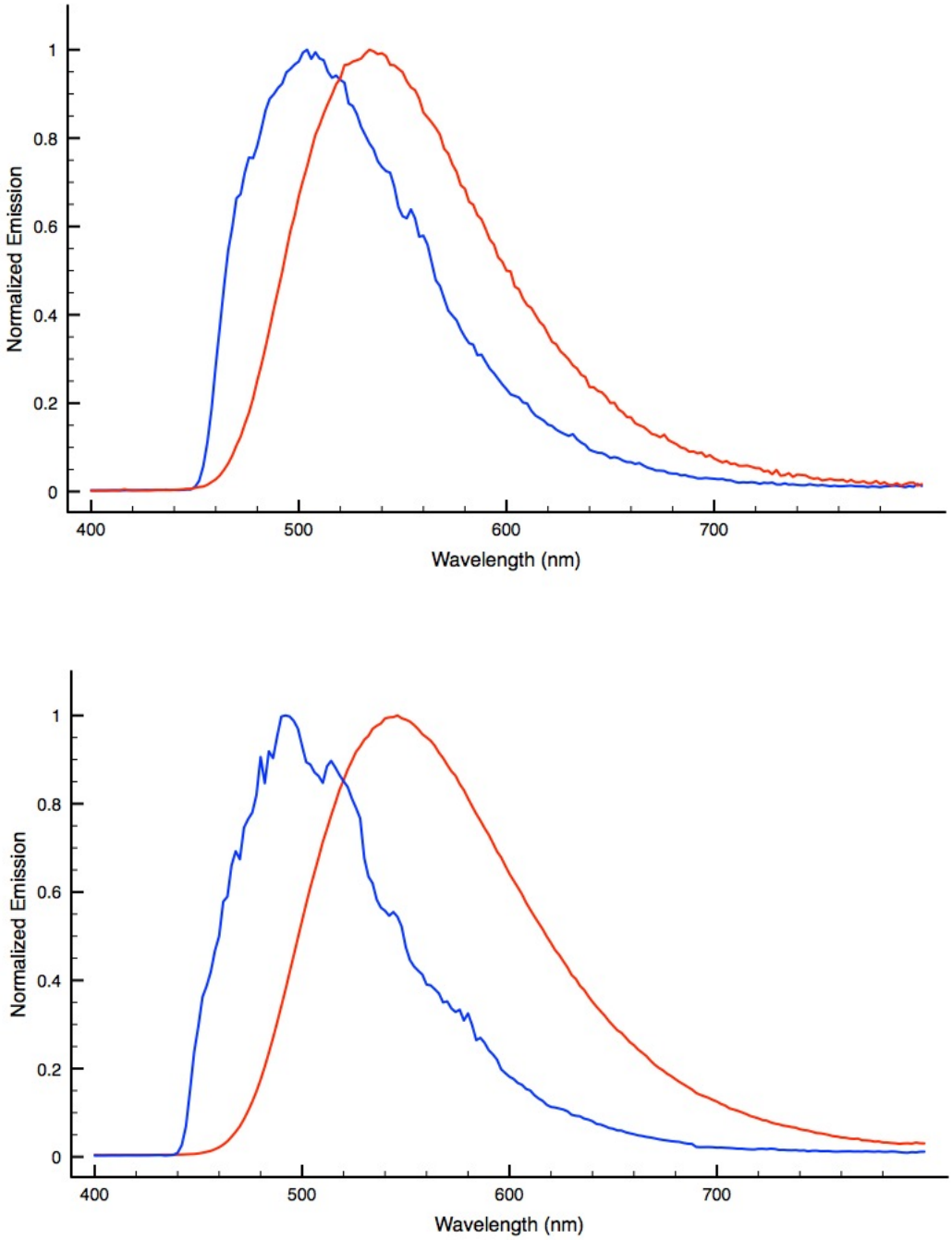

Figure S9. Comparison of the emission spectra obtained from dichloromethane fluid solutions at RT (red trace) and 77 K (blue trace) containing *fac*-[Re(**phen**)$(CO)_3$(**Tmeb**CH_3)][PF_6] (top) and *fac*-[Re(**bipy**)$(CO)_3$(**Tmeb**CH_3)][PF_6], (bottom).

TD-DFT Calculations

Table S1. Summary of TD-DFT data for *fac*-[Re(**phen**)$(CO)_3$(**Tph**CH_3)]$^+$ and its neutral counterpart.

					Group Electron Transition Density (%)		
L=	Transition #	Wavelength (nm)	*f*	Orbital contributions	$Re(CO)_3$	Phen	L
Tph	1	435	0.0432	HOMO->LUMO (97%)	37 → 5	3 → 94	61 → 0
	2	406	0.0071	H-1->LUMO (98%)	91 → 5	6 → 94	3 → 0
	3	399	0.0091	HOMO->L+1 (97%)	37 → 1	3 → 99	61 → 0
	4	383	0.0009	H-3->LUMO (48%), H-2->LUMO (51%)	71 → 5	6 → 94	24 → 0
	5	369	0.0026	H-3->LUMO (12%), H-1->L+1 (79%), H-2->LUMO (6%)	88 → 2	6 → 98	6 → 0
	6	357	0.0796	H-3->LUMO (39%), H-2->LUMO (40%), H-1->L+1 (19%)	75 → 4	6 → 95	19 → 0
	7	347	0.0009	H-3->L+1 (40%), H-2->L+1 (59%)	70 → 1	6 → 99	24 → 0
	8	334	0.0123	H-3->L+1 (58%), H-2->L+1 (38%)	73 → 1	5 → 99	22 → 0
	9	314	0.0051	H-5->LUMO (80%), H-4->LUMO (8%)	6 → 5	75 → 95	19 → 0
	10	310	0.0001	H-4->LUMO (92%)	1 → 5	6 → 94	93 → 0
$TphCH_3$ (N1)	1	393	0.0017	HOMO->LUMO (98%)	89 → 6	6 → 93	5 → 1
	2	373	0.0576	H-2->LUMO (18%), H-1->LUMO (76%)	82 → 6	16 → 93	2 → 1
	3	363	0.0295	H-2->LUMO (76%), H-1->LUMO (11%), HOMO->L+1 (12%)	92 → 6	7 → 94	1 → 1
	4	349	0.0778	H-1->LUMO (11%), HOMO->L+1 (82%)	88 → 2	7 → 98	5 → 0
	5	338	0.0213	H-1->L+1 (91%)	77 → 1	21 → 98	2 → 0
	6	327	0.0068	H-2->L+1 (94%)	94 → 1	6 → 99	1 → 0
	7	314	0.0008	H-3->LUMO (89%), H-6->L+1 (7%)	15 → 6	83 → 93	2 → 1
	8	297	0.0003	H-6->LUMO (35%), H-3->L+1 (63%)	11 → 3	88 → 97	2 → 0
	9	291	0.0248	H-1->L+2 (12%), H-1->L+3 (20%), H-1->L+4 (13%), HOMO->L+2 (16%), HOMO->L+3 (18%), H-1->L+5 (8%)	83 → 24	14 → 22	4 → 54
	10	290	0.0271	H-1->L+2 (14%), H-1->L+3 (18%), HOMO->L+2 (17%), HOMO->L+3 (18%), HOMO->L+4 (11%), HOMO->L+5 (6%)	84 → 23	12 → 21	4 → 55
$TphCH_3$ (N2)	1	389	0.0014	H-1->LUMO (98%)	92 → 6	7 → 93	1 → 0
	2	382	0.0808	HOMO->LUMO (87%), H-2->LUMO (9%)	81 → 6	13 → 94	6 → 0
	3	372	0.0215	H-2->LUMO (89%), HOMO->LUMO (8%)	96 → 6	4 → 93	1 → 0
	4	348	0.0255	HOMO->L+1 (85%), H-1->L+1 (9%)	78 → 1	16 → 99	6 → 0
	5	346	0.0416	H-1->L+1 (84%), HOMO->L+1 (9%)	90 → 1	8 → 99	2 → 0
	6	333	0.0023	H-2->L+1 (98%)	97 → 1	3 → 99	0 → 0
	7	314	0.0055	H-4->LUMO (21%), H-3->LUMO (67%), H-6->L+1 (7%)	7 → 6	54 → 94	40 → 0
	8	300	0.0013	H-1->L+2 (71%), H-1->L+3 (21%)	92 → 5	7 → 2	1 → 93
	9	297	0.0003	H-6->LUMO (38%), H-4->L+1 (15%), H-3->L+1 (45%)	4 → 3	69 → 97	27 → 0
	10	295	0.0334	HOMO->L+2 (62%), HOMO->L+5 (7%), H-4->LUMO (7%)	74 → 15	15 → 9	10 → 76

Table S2. Summary of TD-DFT data for *fac*-[Re(**phen**)$(CO)_3$(**Tmeb**CH_3)]$^+$ and its neutral counterpart.

L=	Transition #	Wavelength (nm)	*f*	Orbital contributions	Group Electron Transition Density (%) Re(CO)$_3$	Phen	L
Tmeb	1	424	0.0513	HOMO->LUMO (95%)	50 → 5	4 → 94	45 → 0
	2	405	0.0124	H-1->LUMO (97%)	90 → 5	6 → 94	3 → 0
	3	389	0.0120	HOMO->L+1 (97%)	50 → 1	4 → 99	46 → 0
	4	382	0.0001	H-2->LUMO (94%)	88 → 5	2 → 94	9 → 0
	5	366	0.0150	H-1->L+1 (93%)	89 → 1	6 → 99	4 → 0
	6	346	0.0476	H-3->LUMO (72%), H-2->L+1 (18%)	52 → 4	8 → 95	40 → 0
	7	346	0.0114	H-3->LUMO (17%), H-2->L+1 (77%)	80 → 2	4 → 98	17 → 0
	8	323	0.0108	H-3->L+1 (91%)	39 → 1	11 → 99	50 → 0
	9	313	0.0336	H-5->LUMO (74%), H-4->LUMO (10%), H-6->L+1 (6%)	8 → 5	67 → 90	25 → 5
	10	308	0.4649	HOMO->L+2 (90%)	48 → 4	7 → 3	45 → 93
TmebCH$_3$ (N1)	1	392	0.0018	HOMO->LUMO (98%)	89 → 6	6 → 93	5 → 1
	2	372	0.0607	H-2->LUMO (20%), H-1->LUMO (74%)	82 → 6	16 → 93	2 → 1
	3	363	0.0350	H-2->LUMO (75%), H-1->LUMO (13%), HOMO->L+1 (10%)	92 → 6	7 → 93	1 → 1
	4	348	0.0785	H-1->LUMO (10%), HOMO->L+1 (83%)	88 → 2	8 → 98	4 → 0
	5	337	0.0218	H-1->L+1 (90%)	77 → 1	22 → 98	2 → 0
	6	327	0.0064	H-2->L+1 (94%)	94 → 1	5 → 98	0 → 0
	7	314	0.0006	H-3->LUMO (79%), HOMO->L+2 (11%), H-4->L+1 (6%)	24 → 6	74 → 82	2 → 12
	8	313	0.0188	H-3->LUMO (10%), HOMO->L+2 (86%)	81 → 2	15 → 11	5 → 87
	9	305	0.0079	H-1->L+2 (90%)	79 → 2	19 → 1	2 → 96
	10	297	0.0001	H-4->LUMO (35%), H-3->L+1 (60%)	14 → 3	85 → 93	1 → 4
TmebCH$_3$ (N2)	1	388	0.0017	H-1->LUMO (96%)	91 → 6	7 → 93	1 → 0
	2	381	0.0793	H-2->LUMO (10%), HOMO->LUMO (84%)	82 → 6	13 → 93	5 → 0
	3	371	0.0230	H-2->LUMO (89%), HOMO->LUMO (9%)	95 → 6	4 → 93	1 → 0
	4	347	0.0293	H-1->L+1 (16%), HOMO->L+1 (78%)	81 → 1	14 → 99	5 → 0
	5	345	0.0381	H-1->L+1 (77%), HOMO->L+1 (16%)	88 → 1	10 → 99	2 → 0
	6	333	0.0023	H-2->L+1 (98%)	97 → 1	3 → 99	0 → 0
	7	318	0.0070	HOMO->L+2 (97%)	79 → 1	15 → 0	6 → 99
	8	316	0.0082	H-1->L+2 (89%), H-1->L+3 (7%)	90 → 1	9 → 3	1 → 96
	9	314	0.0041	H-3->LUMO (84%), H-5->L+1 (6%)	13 → 6	82 → 91	6 → 3
	10	305	0.0002	H-2->L+2 (93%), H-2->L+3 (6%)	97 → 1	3 → 0	0 → 98

Raman Spectroscopy

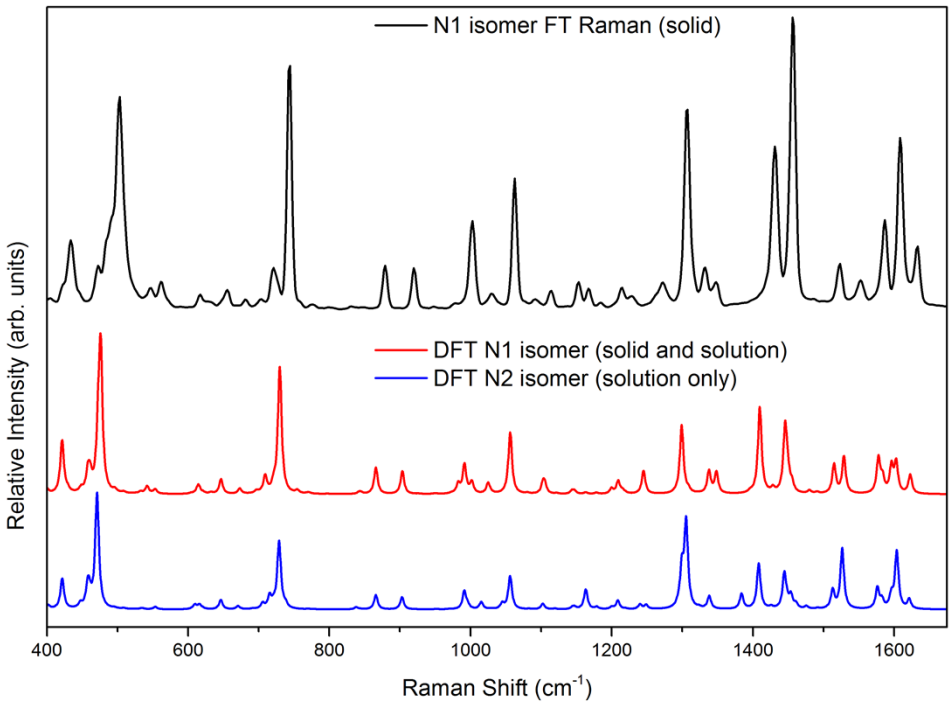

Figure S10. FT-Raman and calculated Raman spectra for *fac*-[Re(**phen**)$(CO)_3$(**Tph**CH_3)]$^+$.

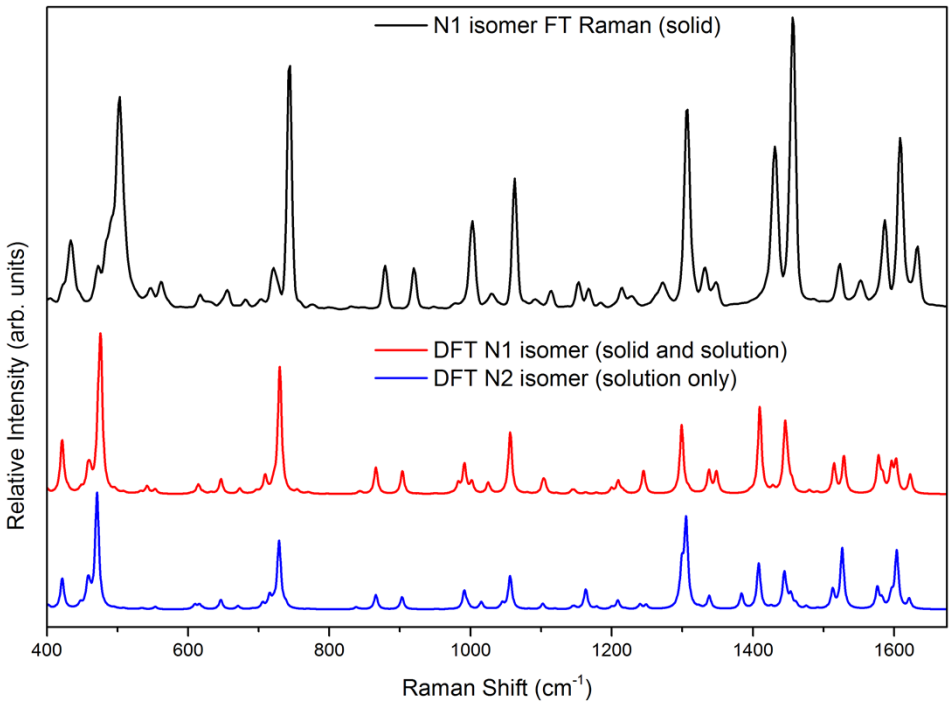

Figure S11. FT-Raman and calculated Raman spectra for *fac*-[Re(**phen**)$(CO)_3$(**Tmeb**CH_3)]$^+$.

Resonance Raman Spectroscopy

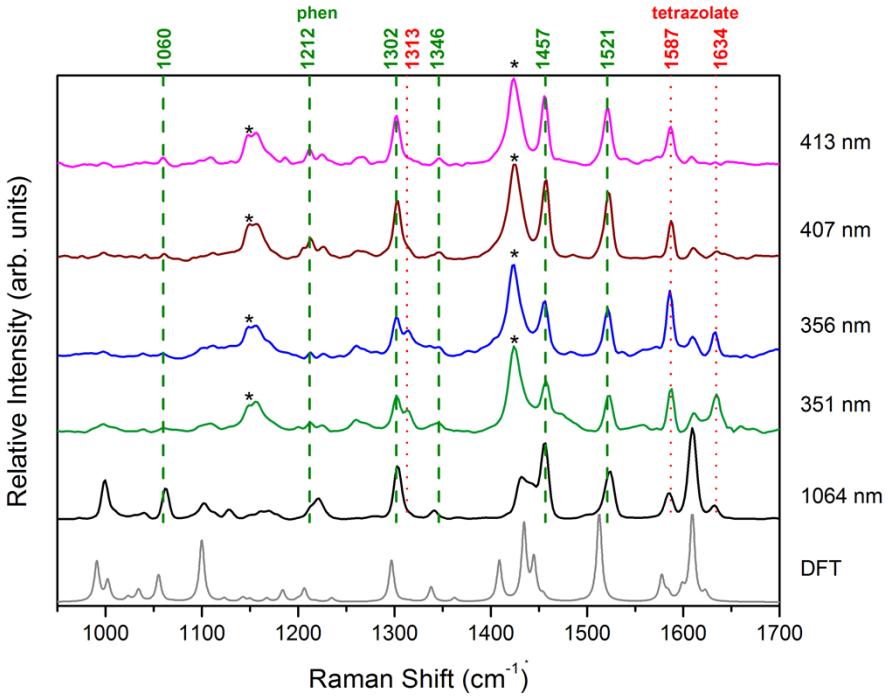

Figure S12. Raman spectra of the neutral *fac*-[Re(**phen**)$(CO)_3$(**Tph**)]. Tetrazolate modes are labelled with dotted lines and **phen** modes with dashed lines.

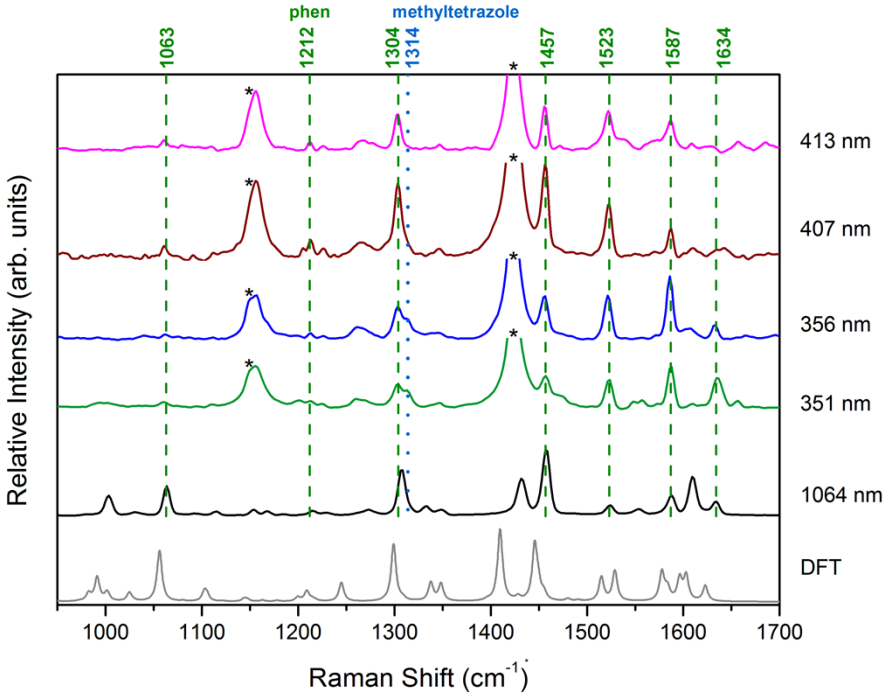

Figure S13. Raman spectra of the cationic *fac*-[Re(**phen**)$(CO)_3$(**Tph**CH_3)]$^+$. Methyltetrazole modes are labelled with dotted lines and **phen** modes with dashed lines.

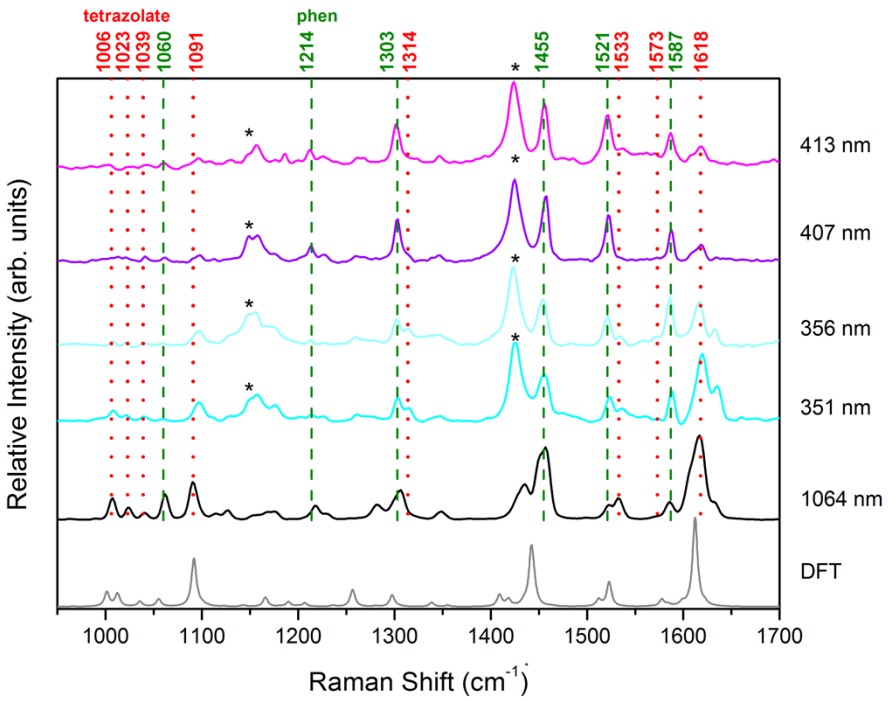

Figure S13. Raman spectra of the neutral *fac*-[Re(**phen**)$(CO)_3$(**Tbdz**)]. Tetrazolate modes are labelled with dotted lines and **phen** modes with dashed lines.

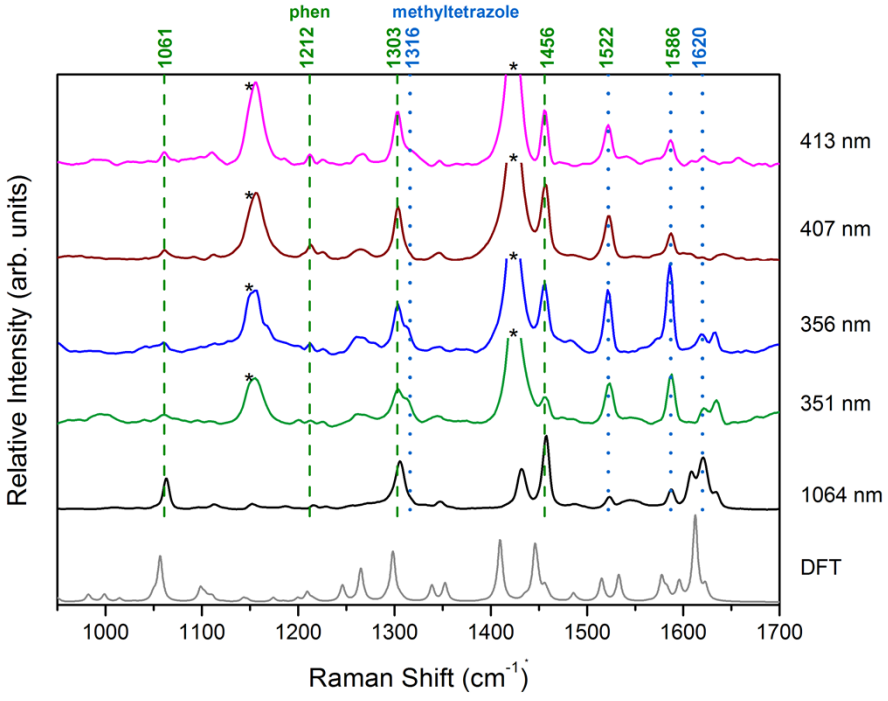

Figure S14. Raman spectra of the cationic *fac*-[Re(**phen**)$(CO)_3$(**Tbdz**CH_3)]$^+$. Methyltetrazole modes are labelled with dotted lines and **phen** modes with dashed lines.

LEEC Performance

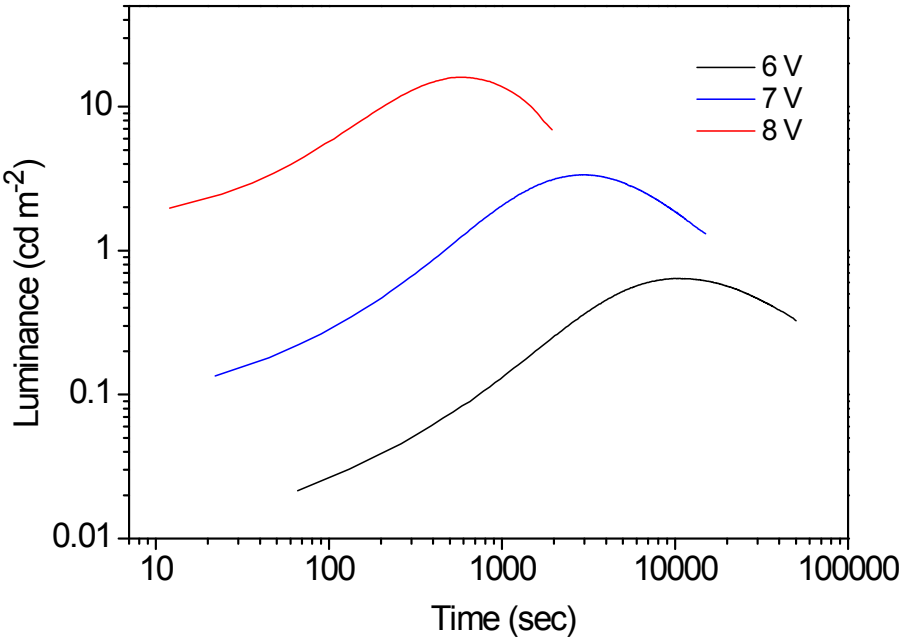

Figure S15. Luminance as a function of time for the LEEC devices having *fac*-[Re(**phen**)$(CO)_3$(**Tph**CH_3)]$^+$ as a single component in the active layer, operating under the bias of 6 (back), 7 (blue) and 8 V (red line).

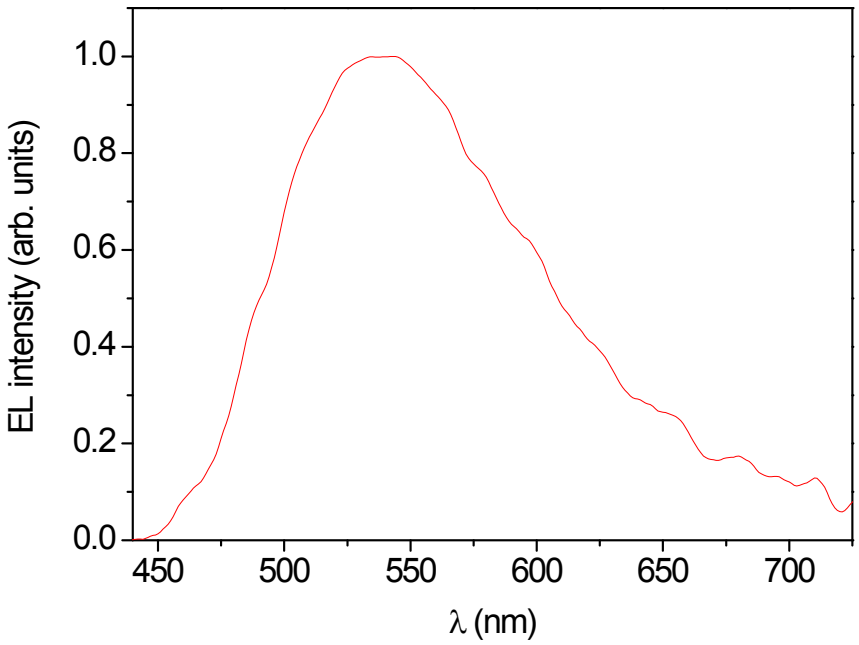

Figure S16. Electroluminescence spectrum of LEEC device having the *fac*-[Re(**phen**)$(CO)_3$(**Tph**CH_3)]$^+$ complex as an emitting layer.